XMM OBSERVATIONS OF THE SUPERSOFT SOURCE RX J0513.9-6951

K. E. McGowan[1], P. A. Charles[2], A. J. Blustin[1], M. Livio[3], D. O'Donoghue[2], and B. Heathcote[4]

[1]Mullard Space Science Laboratory, Holmbury St. Mary, Dorking, Surrey, RH5 6NT, UK
[2]South African Astronomical Observatory, P.O. Box 9, Observatory, 7935, South Africa
[3]STScI, 3700 San Martin Drive, Baltimore, MD 21218, USA
[4]Barfold Observatory, Glenhope, Victoria, 3444, Australia

ABSTRACT

Supersoft X-ray sources (SSSs) are thought to be Eddington limited accreting white dwarfs undergoing surface hydrogen burning, powered by thermally unstable mass transfer from a 1-2 $M_\odot$ companion. However, this model has lacked direct confirmation from observations. The key SSS is RX J0513.9-6951 which has recurrent X-ray outbursts every 100-150 d (lasting $\sim$40 d) during which the optical flux declines by 1 mag. We present the first XMM observations of RX J0513.9-6951 through one of its optical low states. We find that as the low state progresses the temperature and X-ray flux decrease; anti-correlated with the optical/UV emission. As the optical intensity recovers the white dwarf radius increases. The high resolution spectra show evidence of deep absorption features which vary during the optical low state.

Key words: stars; binaries; X-rays.

1. INTRODUCTION

Supersoft sources (SSSs) are a class of X-ray objects with the defining characteristic of extremely luminous emission ($L_X \sim 10^{37} - 10^{38}$ erg s^{-1}) at very soft (< 0.5 keV) X-ray energies. The presence of strong emission lines of H, HeII and higher ionization species in the optical spectra of SSSs indicate that they are low mass X-ray binaries (LMXBs; e.g. van Paradijs & McClintock 1995). However, the nature of the compact object was unclear. "Normal" LMXBs containing neutron star or black hole accretors radiate in a wider energy range at the typical luminosities observed in the SSSs. Using the observed SSS temperatures and bolometric luminosities, van den Heuvel et al. (1992, hereafter vdH92) proposed that the SSSs contain white dwarfs. The near-Eddington luminosities are achieved because the white dwarf accretor is able to sustain steady nuclear burning at its surface. This requires high accretion rates of $> 10^{-7} M_\odot$ yr^{-1}. Such rates are attainable if the donor star is comparable to or more massive than the white dwarf, so that thermally unstable mass transfer occurs (e.g. Paczyński 1971).

While several systems show SSS characteristics, the vdH92 model for the SSSs lacked convincing observational confirmation. Circumstantial evidence in its favour was presented by Southwell et al. (1996; hereafter S96) who showed that the observed bipolar outflow emission lines (Pakull et al. 1993; Cowley et al. 1996) in the transient SSS, RX J0513.9-6951 (hereafter RXJ0513), have velocities comparable to the escape velocity of a massive white dwarf.

MACHO (Alcock et al. 1995) observations of RXJ0513 provided a breakthrough in our understanding of the SSSs. S96 produced a 3.5 year lightcurve of the optical counterpart which revealed recurrent low states (dropping by ~ 1 mag) at quasi-regular intervals (every $100 - 200$ d) and remaining low for $\sim 20 - 40$ d. More importantly, *ROSAT* X-ray detections of RXJ0513 (Schaeidt et al. 1993) are only reported during such optical low states, while no outbursts have been observed during the extensive optical high states i.e. the X-ray and optical states are anti-correlated.

The behaviour observed in RXJ0513 is difficult to reconcile with a regular thermonuclear flash model which is normally accompanied by radius expansion and an increased optical luminosity. Instead, S96 proposed that contraction of the white dwarf from an expanded, Eddington-limited state to a steady shell-burning phase could cause the X-ray outburst. S96 suggested that the contractions could be due to a decrease in the otherwise very high accretion rate, which would also account for the simultaneous optical low states. Of course, the shell luminosity will be even higher in the optically bright state, but the system is then close to the top of the steady burning strip in the $M - M_{WD}$ plane (Nomoto 1982) which means the white dwarf is inflated (Kovetz & Prialnik 1994). Hence most of the shell luminosity would then be emitted in the UV or EUV. This leads to the prediction that, if this model is correct, as the X-ray outburst evolves it will end with its peak emission shifting into the EUV

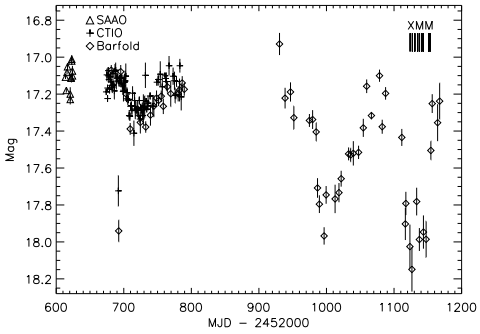

Figure 1. Optical lightcurve of RXJ0513. The observations were obtained at SAAO (triangles), CTIO (crosses) and Barfold Observatory (diamonds). The start times of the X-ray observations are marked.

and UV.

We present *XMM-Newton* observations of RXJ0513 through one of its optical low states. We use these data to examine the validity of the vdH92 paradigm for SSS via the prediction of S96 for the X-ray turn-on and turn-off. If we can confirm directly the vdH92 paradigm for SSS then this will also establish them as one of the strong candidates for the progenitors of type Ia supernovae (see e.g. Livio 1996).

2. OBSERVATIONS AND DATA REDUCTION

We monitored RXJ0513 using ground based optical instruments from 2002 December 5 to 2004 June 11. The optical light curve of RXJ0513 is shown in Figure 1. When RXJ0513 started its ~ 1 mag drop in the optical we triggered our *XMM-Newton* ToO observations. A set of nine X-ray measurements were taken from 2004 April 28 to 2004 May 28. The start of each *XMM-Newton* observation is marked in Figure 1.

We obtained *XMM-Newton* data using the Optical Monitor (OM; Mason et al. 2001), both EPIC instruments, MOS (Turner et al. 2001) and PN (Strüder et al. 2001), and the Resolution Grating Spectrometer (RGS; den Herder et al. 2001). The data were reduced using the *XMM-Newton* SCIENCE ANALYSIS SYSTEM (SAS).

The OM observations were taken using the $UVW2$ filter. We performed the photometry using a $5''$ radius aperture, subtracting a background extracted from a $10''$ aperture offset from the source.

The EPIC observations were taken in timing mode, with the thin filter. The data were filtered to exclude times of high background and events that may have incorrect energies, to include only single photon events for MOS and only single and double photon events for PN, and to include only photons with energies in the range $0.3 - 10$ keV. EPIC spectra were extracted using a region centered

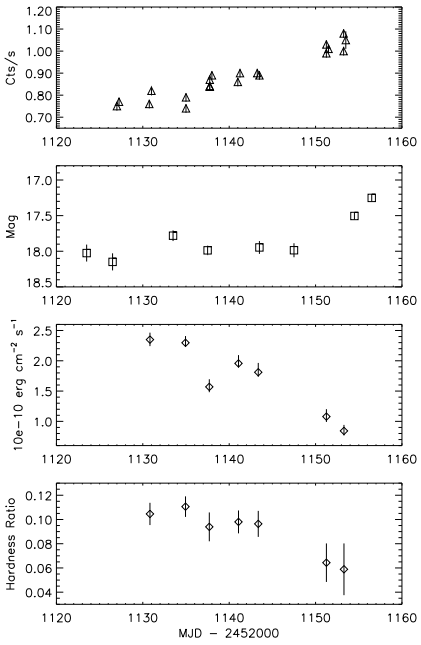

Figure 2. First panel: OM $UVW2$ light curve of RXJ0513, second panel: contemporaneous optical data from Barfold Observatory, third panel: EPIC-PN lightcurve (0.2-10 keV), fourth panel: hardness ratio.

on RXJ0513, corresponding background spectra were extracted using a region of similar size offset from the source position. In each case we created a photon redistribution matrix (RMF) and ancillary region file (ARF). The spectra were regrouped by requiring at least 30 counts per spectral bin. The subsequent spectral fitting and analysis was performed using XSPEC. We extracted source and background light curves from the filtered event files, which had been barycentrically corrected, using the same regions.

We extracted RGS spectra for RXJ0513, subtracting the background using regions adjacent to that containing the source. We combined the RGS1 and RGS2 spectra, including both first and second order data, channel by channel for each observation using the method described by Page et al. (2003). We analysed the RGS spectra using SPEX v2.00 (Kaastra et al. 2002).

3. UV AND OPTICAL LIGHTCURVES

We show in Figure 2 the OM lightcurve of RXJ0513 with contemporaneous ground-based optical data points. The UV intensity is roughly constant at the start of the observations. By MJD 2453137 the UV flux had started to increase, this brightening continued during the remaining observations. By comparing the start of the rise in the UV intensity to the rise in the optical we can see that the UV leads the optical. The lightcurves indicate that the UV brightening is more gradual than in the optical.

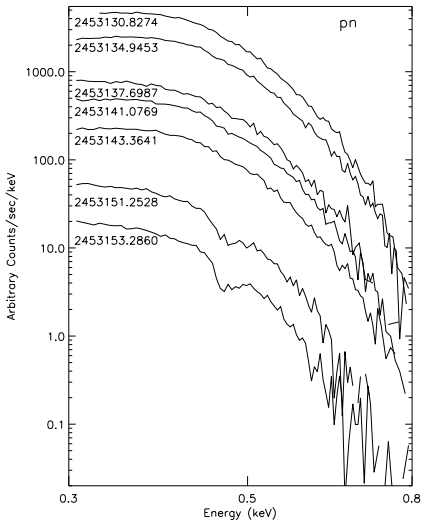

Figure 3. EPIC-PN spectra of RXJ0513 plotted in chronological order of descending time.

We have also plotted the EPIC PN flux in the $0.2 - 10$ keV band. The overall trend for the X-rays during our observing period is a reduction in the X-ray flux. The fourth panel in Figure 2 shows the hardness ratio, which is seen to decrease as the UV and optical intensity increases. We define the hardness ratio for our data as $(0.5 - 0.8)/(0.3 - 0.5)$ keV.

4. LOW RESOLUTION X-RAY SPECTROSCOPY

For the spectral analysis we have only used the higher signal-to-noise PN data. Since no substantial emission is detected at energies > 0.8 keV we extracted the PN spectrum over $0.3 - 0.8$ keV for each observation. In each case we fitted the PN spectra with a blackbody model modified by neutral photoelectric absorption. We modelled all the PN spectra simultaneously and found $N_H = (0.62^{+0.03}_{-0.01}) \times 10^{21}$ cm^{-2} (consistent with the galactic value) and $kT = 43.95^{+0.55}_{-3.45}$ eV. We fit each individual PN spectra, fixing the column density at the value found from fitting all of the PN spectra simultaneously.

We find that the blackbody model does not fit the spectra well implying that a more sophisticated model is required to describe the X-ray emission from RXJ0513. We show in Figure 3 the PN spectra in chronological order. The last two spectra show apparent broad absorption features just below 0.5 keV. Adding one or more absorption edges to the fit (at the observed energy they could originate from C V and/or C VI) does not improve the fit.

While the blackbody model is a poor fit to the spectra, we can however investigate the evolution of the spectra by treating the values obtained as representative of the gross spectral properties. We find that the temperature varies between $38.7 - 47.5$ eV, and the blackbody luminosity between $(1.1 - 2.0) \times 10^{38}$ erg s^{-1}. These values

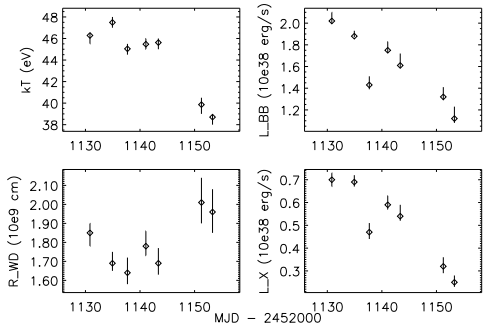

Figure 4. The evolution of kT, blackbody luminosity (L_{BB}), white dwarf radius (R_{WD}) and X-ray luminosity in the 0.2-10 keV band (L_X).

are consistent with those found by Schaeidt et al. (1993) from the *ROSAT* data, as is the value for N_H. We show in Figure 4 the evolution of kT, blackbody luminosity, white dwarf radius and X-ray luminosity in the $0.2 - 10$ keV band, during our observations. As the source starts to emerge from the optical low state we see that the temperature and X-ray luminosity both decrease. This is anticorrelated with the optical and UV emission.

5. HIGH RESOLUTION X-RAY SPECTROSCOPY

The RGS spectra (Figure 5) show evidence of deep absorption features and probably some low significance narrow emission lines. The absorption lines can be identified with transitions from a range of high-ionization ions. Figure 6 shows three individual features plotted in velocity space: C VI Lyα at 33.736 Å, Ar XIII/Ar XIV at 27.463 Å (blended at the RGS spectral resolution), and S XIV at 30.441 Å. It is clear that the lines are blue-shifted and that there are two or more velocity components; the outflow velocity along our line of sight lies between zero and ~ 3000 km s^{-1}.

Figure 6 also indicates that the optical depth of the absorbers increases over the course of the observations. This is seen most clearly in the case of C VI Lyα, which is barely present in the first spectrum, deepens significantly and becomes heavily saturated by the final observation. The velocity structure of the medium is best indicated by the S XIV and Ar XIII/Ar XIV features; although there are some apparent changes over the course of the observations, there appear to be two main velocity components at ~ -1000 km s^{-1} and ~ -3000 km s^{-1} respectively.

Figure 7 shows a comparison of the fifth RGS spectrum (MJD 2453141.5636) with a simple photoionized absorption model to highlight the positions of the major features. The model continuum was chosen to represent the overall shape of the first RGS spectrum (MJD 2453127.0784), which has the least amount of intrinsic ionized absorption and therefore the most continuum visible. The model continuum consists of a Compton-

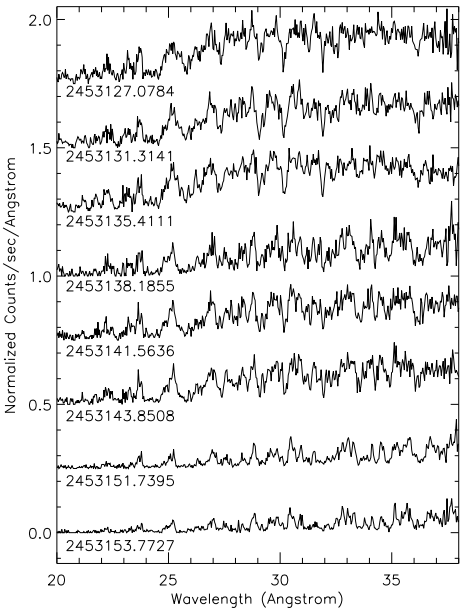

Figure 5. RGS spectra of RXJ0513 plotted in increasing time order from top to bottom.

scattered 70 eV blackbody, with Galactic neutral absorption at the average column derived from the fits to the PN data. The intrinsic ionized absorption is represented using the *xabs* photoionized absorption model in SPEX v2.00 (Kaastra et al. 2002). We find that the depths of the observed features require abundances that are greater than Solar. If the relative elemental abundances in the ionized outflows in RXJ0513 really are several factors above Solar values, this may imply that the outflows contain the products of hot CNO burning.

Comparing the models with the observed spectrum in Figure 7, it is clear that a simple photoionized absorption model is not an adequate representation of the data; this is unsurprising since the assumption of absorption from the ground state would not be valid in a high density medium such as a white dwarf atmosphere. It is also very likely that atomic data are missing or perhaps inaccurate in the current model for various features in the spectrum; identification of ionic species is further complicated by the likelihood that the observed features consist of complicated blends of many different transitions.

Approximating the underlying continuum as a blackbody spectrum is probably still too simplistic; the continuum and intrinsic absorption will need to be modelled self-consistently in order to reach a more accurate understanding of both. Lanz et al. (2005) have shown that a white dwarf atmosphere model is a good representation of the soft X-ray spectrum of the supersoft source CAL 83, although they found no evidence for a high-speed outflow in that source. A white dwarf atmosphere model with the addition of winds and outflows may indeed be required to reproduce the RGS spectra of RXJ0513. Nevertheless, the present model demonstrates clearly that much of the soft X-ray spectral complexity of RXJ0513 is consistent

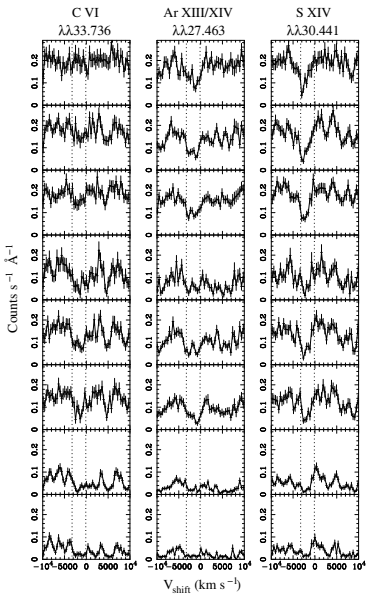

Figure 6. Absorption features from the RGS spectra plotted in velocity space; C VI *Ly*α*, an Ar* XIII*/Ar* XIV *blend and a S* XIV *line at 33.736, 27.463 and 30.441 Å, respectively. The dotted lines at 0 and -3000 km s*$^{-1}$ *mark the approximate boundaries of the features.*

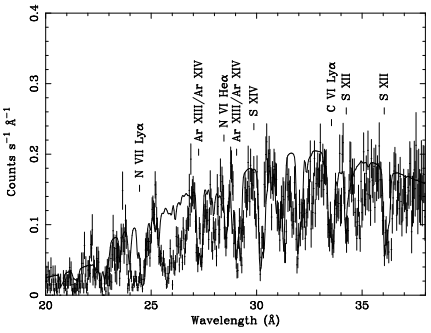

Figure 7. RGS spectrum 5 (MJD 2453141.5636) compared with a simple photoionized absorption model. The positions of various important features are labelled.

with the presence of highly ionized outflowing gas.

6. DISCUSSION

The white dwarf contraction model proposed by S96 is based on the prediction that the rise in the X-rays occurs after the drop in optical luminosity. From the vdH92 model, during the optical bright state the accretion rate is very high ($> 10^{-7}$ M$_\odot$ yr^{-1}). Under these conditions, the white dwarf is slightly inflated, and a large majority of the shell luminosity is likely emitted in the UV. As the accretion rate drops, leading to a reduction in the optical flux, the photosphere contracts slightly (e.g. Kovetz & Prialnik 1994), this raises the effective temperature and hence produces an increase in the X-ray luminosity.

We do not have X-ray observations before the drop, however, previous observations have shown that X-rays are not detected when the source is in its optical high state. Our observations confirm that while RXJ0513 is in its optical low state we see the source in X-rays.

The behaviour of the UV and optical intensity is roughly correlated in the optical low state. However, the UV flux starts to rise before the optical luminosity increases. We find that as the optical low state progresses the X-ray flux decreases, this is anti-correlated with the optical and UV. This implies that as the X-ray outburst is evolving the peak of the emission has moved into the UV, confirming the prediction of the contraction model.

Although our blackbody fits to the PN spectra are poor, the values implied by the fits are indicative of the global evolution of the X-ray emission. We find that the temperature and luminosity decrease during the optical low state. The radius determined from the fits decreases during the first observations. As the optical (and UV) intensity recover the radius increases. In the context of the contraction model (e.g. Hachisu & Kato 2003a,b), the enhanced X-ray flux will irradiate the companion star and, either by inflating material above the secondary's photosphere and causing it to be transferred (e.g. Ritter 1988) or by heating the magnetic spot region (see Parker 1979), will cause the mass transfer rate to increase again. This coincides with the white dwarf photosphere re-inflating, hence the radius gets larger, and the X-ray flux decreases again. Therefore, as RXJ0513 returns to its optical high state the source is once again not observable in X-rays.

Our spectral fits to the PN data indicate that a more complicated model is needed to describe the X-ray emission. The higher spectral resolution data from the RGS reveal the existence of highly ionized gas outflowing along our line of sight at speeds of up to 3000 km s^{-1}, with multiple velocity components that evolve over time. The optical depth of the ionized absorption appears to increase over the course of the RGS observations; this is borne out by the lower-resolution PN spectra, in which deep absorption features become apparent in the final two spectra. The presence of this absorption partly explains why the blackbody fits are so poor.

There are a variety of possible causes for the increase in optical depth of the intrinsic absorption. We could be viewing the system close to pole-on (i.e. low inclination) through the (presumably) bipolar outflow, and the intrinsic covering factor of the outflow is changing. Possible explanations for this include the effects of a magnetic cycle of the optical star, the expansion of the white dwarf or the system precessing with respect to our line of sight.

Alternatively, it might not be the bipolar outflow we are seeing, but actually the process of expansion of the white dwarf surface itself, as highly ionized nova by-products stream out from the white dwarf surface and gradually build into an optically-thick inflated surface, confined by the gravity of the white dwarf. The increase in optical/UV radiation would then occur as the 'intrinsic' X-rays are down-scattered in the increasingly optically thick outer inflated layer of the white dwarf. The apparently anomalous abundances of Sulphur, Argon and Nitrogen in the ionized outflow may indeed imply that the gas originated in the nova nucleosynthesis. The abundances may be modified in the atmosphere of the steady nuclear burning white dwarf via hot CNO burning (cf. CNO abundances for CAL83 using NLTE model atmospheres, Lanz et al. 2005).

We find that the RGS spectra deviate from the blackbody approximation at $24 - 27$ Å this may be due to effects of carbon transitions in this range due to a white dwarf atmosphere. A white dwarf atmosphere with an effective temperature as deduced from the blackbody fits to the PN data shows that with increasing gravity (white dwarf mass) above the C VI edge the atmospheric density increases. This shifts the ionization equilibrium toward a lower degree of ionization, causing the emission edges to turn to absorption (e.g. Hartmann & Heise 1997). For the same gravity the energy of the C absorption shifts to lower energies due to a change of the ionization state of C. Thus the C V–VI absorption due to the white dwarf stellar atmosphere may be at least partly responsible for the disagreement found from the blackbody approximation (see Paerels et al. 2001; Rauch et al. 2005).

The existence of an ionized absorber in the X-ray spectrum of RXJ0513 seems plausible as the absorption lines found in the RGS spectrum of the fifth (and other) observations of the source require a shift due to a velocity up to 3000 km s^{-1} which is consistent with the escape velocity of a massive white dwarf. In RXJ0513 the existence of absorption structures which cannot be explained by a photoionized absorber model (especially those between $24 - 27$ Å) indicates that the absorption takes place in a high-density medium. This would be consistent with an origin in a white dwarf atmosphere.

The spectral model we constructed for the fifth RGS spectrum in the series does reproduce many spectral features due to the ionized outflow in RXJ0513. The ionization structure for such an ionization parameter would be consistent with that of the outflowing version of model 8 in Kallman & McCray (1982), which models gas photoionized by a blackbody emitter. We can estimate the mass outflow rate assuming the accretion is slightly super-Eddington. The Eddington luminosity is $L_{Edd} \sim 1.2 \times 10^{38}\ M/\ \mathrm{M}_\odot$ erg s^{-1} (e.g. Grimm et al. 2002). As $\dot{M}_{out}\nu = L_{Edd}/c$ (see King & Pounds 2003), we determine with $M = 1\ \mathrm{M}_\odot$, $L_{Edd} = 1.2 \times 10^{38}$ erg s^{-1}, and $\nu = 3000$ km s^{-1}, $\dot{M}_{out} = 2.1 \times 10^{-7}\ \mathrm{M}_\odot\ \mathrm{yr}^{-1}$. This value for the mass outflow rate is consistent with the wind mass loss rate estimated by Hachisu & Kato (2003b) for RXJ0513.

We can also directly compare the physical parameters inferred from the observational data of the low-state egress of RXJ0513 with the parameters predicted by the model of Hachisu & Kato (2003b), for the high/low state transitions of RXJ0513. The evolution of the blackbody temperature inferred from the EPIC-PN data follows roughly

the evolution of the temperature as inferred by Hachisu & Kato (2003b), although the temperatures and the radii inferred from the observations are about 25% higher and a factor of 2 smaller, respectively. One prediction of the Hachisu & Kato (2003b) model are winds from the white dwarf with a wind mass-loss rate of $\sim 10^{-7}$ $M_\odot$ yr^{-1} during this part of the lightcurve. We can estimate the optical depth of such a highly ionized wind due to Thomson scattering opacity assuming an outflow velocity of 3000 km s^{-1} and a radius of 10^9 cm. For a wind mass-loss rate of 10^{-7} $M_\odot$ yr^{-1} we calculate an optical depth of 1 which is sufficient to obscure the soft X-ray source during the low-state egress.

7. SUMMARY

We have presented a series of *XMM-Newton* EPIC-PN and RGS observations during the late phase (onset of egress) of an optical low-state of the supersoft X-ray source RXJ0513. Simultaneous *XMM-Newton* OM and long-term ground based optical monitoring are also reported. We have derived the evolution of the fluxes in the observed bands and the evolution of the X-ray spectral parameters from a blackbody spectral fit to the EPIC-PN data. We find that the temperature and luminosity decrease, and an indication of an increase in the radius of the blackbody emitter with time. During the late phase of the optical low-state we find broad spectral dips in the EPIC-PN spectra just below 0.5 keV. The RGS spectra show deep absorption features (e.g. C VI, Ar XIII/XIV, S XIV) which deepen with time and in addition some weak emission lines. We model the RGS spectra with a Compton-scattered 70 eV blackbody with Galactic neutral absorption and additional intrinsic ionized absorption due to outflowing gas using a photoionized absorption model. Our spectral model for the fifth RGS spectrum, which was taken in the deepest part of the optical low state, requires velocities of the outflowing gas of up to 3000 km s^{-1}. We find that the spectral model lies above the observed spectrum in the $24 - 27$ Å regime which is likely to be due to effects related to the white dwarf atmosphere.

ACKNOWLEDGMENTS

This work is based on observations obtained with *XMM-Newton*, an ESA science mission with instruments and contributions directly funded by ESA Member States and NASA.

REFERENCES

Alcock C., et al. 1995, Phys. Rev. Lett., 74, 2867

Cowley A. P., Schmidtke P. C., Crampton D., Hutchings J. B. 1996, In: eds van den Heuvel E. P. J., van Paradijs J., Proc. IAU Symp. 165: Compact Stars in Binaries, Kluwer, Dordrecht, p. 439

den Herder J. W., et al. 2001, A&A, 365, L7

Grimm H. -J., Gilfanov M., Sunyaev R. 2002, A&A, 391, 923

Hachisu I., Kato M. 2003a, ApJ, 590, 445

Hachisu I., Kato M. 2003b, ApJ, 588, 1003

Hartmann H. W., Heise J. 1997, A&A, 322, 591

Kaastra J. S., Mewe R., Raassen A. J. J. 2002, in ESA SP-488, New visions of the X-ray Universe in the XMM-Newton and Chandra Era, ed. F. Jansen, electronic proceedings

Kallman T. R., McCray R. 1982, ApJS, 50, 263

King A. R., Pounds K. A. 2003, MNRAS, 345, 657

Kovetz A., Prialnik D. 1994, ApJ, 424, 319

Lanz T., Telis G. A., Audard M., et al. 2005, ApJ, 619, 517

Livio M. 1996, in: ed Greiner J., Lecture Notes in Physics 472: Supersoft X-ray Sources, Springer-Verlag, p. 183

Mason K. O., et al. 2001, A&A, 365, L36

Nomoto K. 1982, ApJ, 253, 798

Paerels F., Rasmussen A. P., Hartmann H. W., et al. 2001, A&A, 365, 308

Paczyński B. 1971, ARAA, 9, 183

Page M. J., Davis S. W., Salvi N. J. 2003, MNRAS, 343, 1241

Pakull M. W., et al. 1993, A&A, 278, L39

Parker E. N. 1979, Cosmical Magnetic Fields (Oxford: Clarendon)

Rauch T., Werner K., Orio M. 2005, Proceedings ITAMP Workshop: X-ray Diagnostics for Astrophysical Plasmas: Theory, Experiment, and Observation. 2004 November 15-17 Cambridge, USA, (astro-ph/0501012)

Ritter H. 1988, A&A, 202, 93

Schaeidt S., Hasinger G., Trümper J. 1993, A&A, 270, L9

Southwell K. A., Livio M., Charles P. A., et al. 1996, ApJ, 470, 1065

Strüder L., et al. 2001, A&A, 365, L18

Turner M. J. L., et al. 2001, A&A, 365, L27

van den Heuvel E. P. J., Bhattacharya D., Nomoto K., Rappaport S. A. 1992, A&A, 262, 97

van Paradijs J., McClintock J. E. 1995, In: eds Lewin W. H. G., van den Heuvel E. P. J., X-ray Binaries, Cambridge Univ. Press, Cambridge, p. 58